

III. Thermal Properties and Ion Transport

Rigid models made of wooden balls and metal rods are used to represent crystal structures, but the atoms in a real solid are in ceaseless motion, oscillating rapidly about their equilibrium sites. As Dame KATHLEEN LONSDALE wrote, "a crystal is like a class of children arranged for drill, but standing at ease, so that while the class as a whole has regularity both in time and space, each individual child is a little fidgety" [1].

In a crystal this fidgetiness usually amounts to a few percent of the interatomic distance. For the elements listed in Table 6, the vibration amplitudes are 3–7% of the nearest neighbor distances. As might be expected, the vibrations are largest for soft materials such as lithium and lead, and smallest for diamond.

Vibration amplitudes increase with temperature, but not very rapidly. The root-mean-square vibration amplitude of aluminum increases from 0.057 Å at 10 °K to 0.152 Å at 600 °K. Motion continues to low temperatures because of the presence of zero point energy.

Atoms do not vibrate with equal amplitude in all directions. Magnesium and zinc crystallize in the hexagonal close-packed structure with twelve neighbors around each atom, six in the same (001) layer, three in the layer above, and three below. The packing in magnesium is almost

Table 6. Debye temperature Θ and root-mean-square vibration amplitudes at room temperature [2]

Element, structure, and interatomic distance (Å)			Θ (°K)	$\sqrt{U^2}$ (Å)
Al	FCC	2.86	395	0.101
Au	FCC	2.88	175	0.084
Cu	FCC	2.56	314	0.084
Li	BCC	3.04	316	0.209
Mg	HCP	3.20, 3.21	320	c 0.125
				$\perp c$ 0.130
Pb	FCC	3.50	70	0.206
Zn	HCP	2.67, 2.91	250	c 0.153
				$\perp c$ 0.091
C	D	1.54	1860	0.05
Si	D	2.34	550	0.075

ideal with nearly equal interatomic distances, and thermal vibrations are nearly isotropic (Table 6). In zinc, the c/a ratio exceeds the ideal value (1.633) so that the Zn–Zn distances within a close-packed plane are shorter than those between atoms in adjacent layers. As a result atoms can vibrate more easily along c than perpendicular to c where atomic motion is more restricted.

Thermal vibrations in cubic crystals are generally described as isotropic but there is no reason why this should be so. In rocksalt, for instance, atomic bonds are parallel to the six equivalent [100] directions. Vibrations in these directions probably differ from those in [111] directions, although this has yet to be proven.

For diatomic compounds the lighter of the two atoms generally vibrates with the larger amplitude. Thermal vibration amplitudes estimated from X-ray diffraction intensities for LiH show that H^- vibrates more than Li^+ because it is lighter. Measurements on LiF, NaF, NaCl, KCl, and CaF_2 verify this result [2].

In organic molecular crystals where C, N, and O all have about the same atomic weight, the atoms near the perimeter of the molecule usually undergo larger vibrations than those near the center where the bonding is stronger.

1. Lattice Vibrations

The nature of lattice vibrations in crystals can be illustrated with a one-dimensional rocksalt structure (Fig. 21). A row of alternating cations and anions has a lattice parameter $2a$, where a is the interatomic distance. Masses of the positive and negative ions are represented by M and m , respectively. For the purposes of argument, we assume M is greater than m .

Equations of motion for a one-dimensional NaCl structure have been derived by BRILLOUIN [3] under the assumption that interactions take place between nearest neighbors only. The force on the n th particle is given by $k(y_{n+1} - y_n) + k(y_{n-1} - y_n)$ where y_n , y_{n+1} , and y_{n-1} are the displacements of n th particle and its nearest neighbors from their equilibrium sites, and k is the force constant. Plane wave solutions to the equations of motion lead to two ranges of allowed angular frequencies:

$$\omega^2 = k \left(\frac{1}{M} + \frac{1}{m} \right) \pm k \sqrt{\left(\frac{1}{M} + \frac{1}{m} \right)^2 - 4 \frac{\sin^2 Ka}{Mm}}.$$

The angular frequency of a lattice vibration is ω with wave number $K = 2\pi/\lambda$. As shown in Fig. 22, the $\omega(K)$ curve for a diatomic chain has

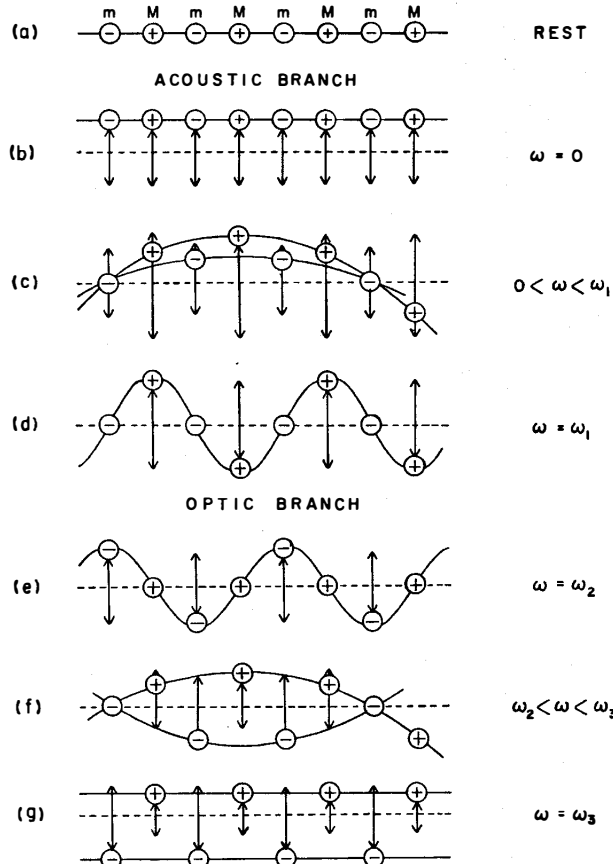


Fig. 21 a-g. Motion of particles in a diatomic chain. Frequencies correspond to those in Fig. 22

two branches. The low frequency branch extending from $\omega=0$ to $\omega = \sqrt{2k/M}$ is called the *acoustical* branch because the frequencies are of the same order as acoustical or supersonic vibrations. Allowed frequencies in the upper branch ($\omega_2 < \omega < \omega_3$) extend into the infrared, hence it is called the *optical* branch.

Particle motions are illustrated in Fig. 21. At very low frequencies, all particles vibrate in phase with equal amplitudes. As the frequency increases, the amplitude of the light atoms decreases, and they remain at

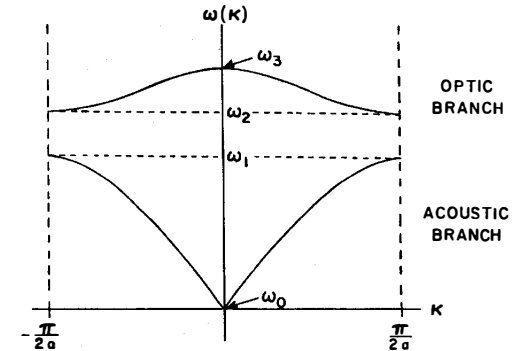


Fig. 22. Allowed vibration frequencies for a diatomic chain of alternating large and small masses, M and m . Angular frequency ω is plotted as a function of wave number K . The acoustic branch extends from $\omega=0$ to $\omega_1 = \sqrt{\frac{2k}{M}}$, and the optic branch from $\omega_2 = \sqrt{2k/m}$ to $\omega_3 = \sqrt{2k\left(\frac{1}{M} + \frac{1}{m}\right)}$. Frequencies between ω_1 and ω_2 are not allowed

rest for the limiting wavelength ($\lambda = 4a$) in the acoustic branch, while the heavy atoms continue to oscillate. Particle motions for frequencies at the bottom of the optic branch are very similar to those at the top of the acoustic branch. For low-frequency vibrations in the optic branch, all heavy particles are at rest while light particles move in alternate directions ($\lambda = 4a$). As the wavelength increases, the amplitude of the heavy particle increases, though the vibration amplitude of the lighter particles is always greater in the optic branch. For infinite wavelengths, the heavy and light particles oscillate in opposite directions. Vibrations of this type can be excited by electromagnetic waves because electric fields drive positive and negative ions in opposite directions, giving rise to infrared absorption in NaCl and other ionic crystals.

The lattice vibrations discussed here are those of a *diatomic* chain for which there is one acoustic branch and one optic branch. For a *monatomic* chain, the optic branch disappears leaving just the acoustic branch. More complicated chains with N atoms per cell have an acoustic branch and $(N-1)$ optical branches.

2. Thermal Properties

Specific heat is the amount of heat required to raise the temperature of one mole of a substance by 1°K . In most solids the atoms vibrate about their equilibrium positions but there are no rotational degrees of

freedom. Classically, each vibrational degree of freedom involves both potential and kinetic energy giving a thermal energy of kT per degree of vibrational freedom. Since there are three independent directions, the average vibrational energy is $3kT$. For N atoms, the internal energy $U = 3NkT$ and the specific heat is

$$C_v = \left(\frac{\partial U}{\partial T} \right)_v = 3Nk.$$

An element contains $N_0 = 6.023 \times 10^{23}$ atoms per mole, giving $C_v = 3N_0k = 6 \text{ Cal/}^\circ\text{K}$ per mole. Thus the classical result depends only on the number of atoms, and is independent of the atomic species, chemical bonding, and crystal structure. Near room temperature and above, measured values agree well with theory. Some typical values for solid elements are Al 6.0, Cu 5.7, Ag 5.8, and Pb 6.2 Cal/ $^\circ\text{K}$ mole.

Diatomic solids contain $2N_0$ atoms per mole, doubling the specific heat. The specific heat of sodium chloride at room temperature is 12.0 Cal/ $^\circ\text{K}$ mole. For a mole of triatomic CaF_2 , the observed value is 17.1, in accordance with the number of atoms per mole.

At lower temperatures, the specific heat approaches zero at 0 $^\circ\text{K}$. Debye developed a theory which describes the temperature dependence of C_v in which the shape of the curve is governed by a characteristic temperature Θ_D , the Debye temperature. For substances with small Θ_D , C_v increases rapidly with temperature, leveling off at the classical value well below room temperature. The characteristic temperature is controlled by the elastic constants and chemical bonding (Table 6). Soft metals have low Debye temperatures: Pb 70 $^\circ\text{K}$, Cd 168 $^\circ\text{K}$. The Θ_D values for ionic crystals are somewhat higher (NaCl 280 $^\circ\text{K}$, CaF_2 475 $^\circ\text{K}$) but much less than diamond (1860 $^\circ\text{K}$).

Anisotropic crystals show unusual behavior at low temperatures, where the specific heat of most simple structures is proportional to T^3 . Layer structures such as arsenic and antimony follow a T^2 dependence while selenium and other chain structures show a linear relation between specific heat and temperature.

Benzol and other molecular crystals have peculiar specific curves because chemical bonding within a molecule is much stronger than between molecules. As a result, the intermolecular vibrations are much easier to excite than the internal vibrations within a single molecule, and the material behaves as if it had two characteristic temperatures.

The specific heat of some molecular solids are unusually large because of rotational motions. The onset of molecular rotations is accompanied by large changes in C_v .

3. Thermal Conductivity

Benjamin Franklin observed that the metal lock on his desk felt colder than wood because of the different powers possessed by metal and wood for conducting heat. If different portions of a solid are at different temperatures, thermal energy is transported from the warmer region to the cooler region. The thermal conductivity coefficient provides a quantitative measure of the rate at which thermal energy is transported along the thermal gradient.

Thermal conductivity coefficients k relate the heat flux \dot{Q}/A (cal/sec-m²) to temperature gradient $\Delta T/\Delta X$ ($^\circ\text{K}/\text{m}$): $\frac{\dot{Q}}{A} = k \frac{\Delta T}{\Delta X}$, where A is the

cross-sectional area and ΔX the sample thickness. There are two principal contributions to thermal conductivity, from free electrons and from phonons. The latter occur in all solids while free electron movement is appreciable only in metals. Hence metals generally have larger room-temperature conductivities (10–100 cal/m sec- $^\circ\text{K}$) than insulators (~ 1 cal/m sec- $^\circ\text{K}$). Among insulators, amorphous solids have smaller conductivities than crystals because the phonon waves are scattered more often in an aperiodic structure. Gemologists distinguish glass imitations from crystalline gems by touching the stone with the tongue. Glass feels warm compared to crystal because of its smaller thermal conductivity. The thermal conductivity of glass is usually smaller than that of a crystal of similar composition because of phonon scattering by the irregular structure. At ordinary temperatures the mean free path is of the order of 10 Å, about the size of silicate rings in the disordered structure. Long-wavelength (low-energy) phonons are not scattered as effectively, so the mean path length increases at very low temperatures.

Radiation damage has a similar effect. When quartz is exposed to neutrons, the thermal conductivity is suppressed and approaches the values observed for silica glass. Chemical impurities and isotopes also promote phonon scattering.

The thermal conductivity of a solid can be expressed as the sum of lattice and electronic components: $k = k_L + k_e$. For nonmetals, the electronic components is negligible, and $k \cong C v l/3$, where C is the contribution of the lattice waves to the specific heat, v is the wave velocity and l the mean free path. At high temperatures, k_L varies inversely with T because the mean free path is shortened by thermal vibrations. As the temperature is lowered, thermal conductivity goes through a maximum and then approaches zero as T goes to 0 $^\circ\text{K}$. The low temperature behavior is governed by imperfections and by sample dimensions.

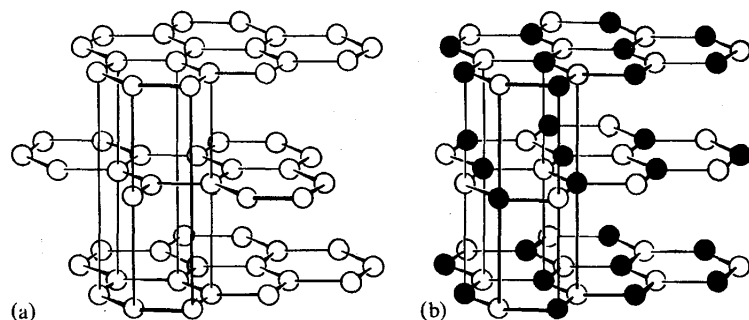


Fig. 23 a and b. Crystal structures of (a) graphite and (b) boron nitride. Both are layer structures with highly anisotropic physical properties. The stacking of the layers is slightly different in the two structures

Metals contain many free electrons so that the electronic thermal conductivity predominates over the lattice contribution. The electric conductivity σ and thermal conductivity k are proportional to one another since both are controlled by the free electron concentration. The Weidmann-Franz law ($k/\sigma T = L$) works well for many metals, with the constant L near its theoretical value of $2.44 \times 10^{-8} \text{ V}^2/\text{K}^2$.

For glasses and cubic crystals k is scalar, but depends on direction for lower symmetries. Among anisotropic materials, chain and layer structures show greater conductivity in the directions of closest bonding. Tellurium crystallizes in spirals parallel to the trigonal c -axis and the ratio of conductivities parallel and perpendicular to the chains is 1.5. In the layer structure of graphite, the conductivity is four times greater within the layer than perpendicular to it. Because of this, graphite and boron nitride are used as heat shields in space vehicles (Fig. 23).

Diamond has a higher thermal conductivity between -200°C and 1000°C than any other material. Heat is easily transferred because of the high Debye temperature. There is relatively little thermal and impurity scattering of the phonons. Natural Type IIa diamond (those that transmit light at 2500 \AA) is a far better conductor of heat than metallic copper, which is normally used for mounting solid state devices. This variety of diamond has a low nitrogen content, and is abundant in certain South African mines. Mounting the electronic device on diamond gives an excellent heat sink. In this way diodes can be operated at higher outputs and lower junction temperatures. The use of diamond heat sinks also makes it possible to operate GaAs junction lasers at normal temperatures.

Thermal conductivity is an important parameter in carbide tool materials where k ranges from about $5\text{--}25 \text{ cal/m sec}^\circ\text{K}$. There exists a direct correlation between k and the tool-chip contact length which controls various mechanisms of the chip formation process. Decreasing the thermal conductivity of the tools material decreases both the normal and tangential components of the cutting force, as well as decreasing crater wear-rate on the rake face. It is possible to develop tool materials with better machinability by reducing thermal conductivity.

Low frequency phonons dominate the heat transport and storage capacity of materials at very low temperatures. Appreciable control of thermal conductivity by external electric fields is therefore possible in soft-mode materials. Strontium titanate (SrTiO_3) exhibits soft-mode behavior at low temperatures where the TiO_6 octahedra undergo rotational motions about $[001]$. At 5°K an electric field of 23 kV/cm induces a five fold increase in the thermal conductivity of SrTiO_3 . Rapid thermal switches could be constructed from soft-mode materials with field-tunable thermal conductivity [4].

4. Ultrasonic Attenuation

In many insulators the attenuation of sound waves of microwave frequencies is a result of energy transfer from the sound wave to thermal phonons. A simple correlation exists between sound attenuation and thermal conductivity: losses at microwave frequencies increase with thermal conductivity. Germanium and silicon have thermal conductivities $k \sim 12 \text{ cal/m sec}^\circ\text{K}$ and rather high attenuation near 20 dB/cm . Al_2O_3 , TiO_2 , MgO , and other oxides are more promising materials for sound propagation with much lower attenuations of 0.2 to 0.6 dB/cm . Thermal conductivities are much smaller in the oxides, $1\text{--}4 \text{ cal/m sec}^\circ\text{K}$.

Measurement of ultrasonic attenuation in a number of materials at room temperature has demonstrated that the Akhiezer mechanism dominates in good dielectric crystals. Akhiezer attenuation arises because the frequencies of thermal phonons are modified by the strain field of the ultrasonic wave through the lattice anharmonicity. The materials with lowest ultrasonic losses are those of low atomic numbers, high Debye temperatures, and complex structures. Topaz ($\text{Al}_2\text{SiO}_4\text{F}_2$), beryl ($\text{Be}_3\text{Al}_2\text{Si}_6\text{O}_{18}$), and tourmaline ($\text{NaMg}_3\text{Al}_6\text{B}_3\text{Si}_6\text{O}_{27}(\text{OH})_4$) satisfy these criteria, and all are found to exhibit very low losses [5,6]. Tourmaline is piezoelectric, and may prove useful as a high-frequency transducer or as a surface-wave medium because of its low ultrasonic attenuation.

5. Thermal Expansion

The china cup that cracks when filled with hot water is a familiar example of thermal shock. Thermal stresses result from the differential thermal expansion caused by temperature gradients. Such stresses are directly proportional to the thermal expansion coefficient α , defined as the change in length per unit length per degree rise in temperature, $\alpha = \frac{1}{\Delta T} \frac{\Delta l}{l}$. Since strain is a second rank tensor and temperature a scalar, the thermal expansion coefficients also constitute a second rank tensor. Three coefficients are required for crystals in the orthorhombic monoclinic, or triclinic systems, two in trigonal, tetragonal, and hexagonal crystals, and one in cubic, and amorphous materials.

The crystal structures of MgO, BeO, Al₂O₃, MgAl₂O₄, and BeAl₂O₄ are all based on close-packed oxygen lattices and all exhibit fairly large thermal expansion coefficients, $8\text{--}10 \times 10^{-6}/^\circ\text{C}$. The effect of temperature is to increase thermal vibration, and in close-packed structures this results in atoms vibrating against one another since they are in close contact. The situation is more complicated in open structures where two additional effects can occur. The atoms can vibrate anisotropically toward open spaces in the structure, resulting in low thermal expansion coefficients. Thus many open structure oxides have small thermal expansion coefficients—compounds like spodumene ($2 \times 10^{-6}/^\circ\text{C}$) are therefore useful because of their thermal shock resistance. Secondly, there can be cooperative rotational effects which lead to a rapid change in thermal expansion coefficients with temperature, as in quartz. The small expansivity of silica glass ($< 10^{-6}/^\circ\text{C}$) has been attributed to the fact that the densities are low and also that cooperative rotations are not possible in amorphous structures.

Strong interatomic forces are associated with low thermal expansion, weak forces with high expansion. Many structures contain a mixture of strong and weak bonds, so that atoms are tightly-packed in some places, and loose in others, as illustrated schematically in Fig. 24. Structural units of length l_1 , with a small thermal expansion coefficient α_1 , are separated by a soft matrix having a large expansion coefficient α_2 . If l_2 is the distance between building blocks, the overall thermal expansion coefficient is given by

$$\frac{l_1\alpha_1 + l_2\alpha_2}{l_1 + l_2}.$$

A model such as this could be used in predicting and correlating thermal expansion coefficients for layer and chain materials, or for aniso-

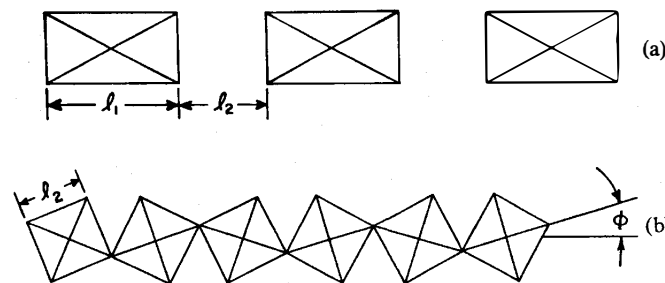


Fig. 24a and b. Two hypothetical models illustrating thermal expansion in (a) anisodesmic structures and (b) open framework structures [7]

desmic compounds. The values of α_1 and α_2 could be estimated from other materials.

A second concept important to the microscopic understanding of thermal expansion is that of tilting (Fig. 24). In open structures, the polyhedra may rotate causing unusually large or unusually small expansion coefficients. Giving a contribution of

$$\frac{1}{l} \frac{dl}{dT} - \tan \Phi \frac{d\Phi}{dT}.$$

The first term is associated with the expansion of the square itself, the second with the crumpling of the framework. In quartz, the decrease angle Φ accounts for more than half of the thermal expansion.

Framework silicates such as quartz and cristobalite are in a partially collapsed structure at room temperature. At high temperatures, the SiO₄ tetrahedra rotate to an open fully-expanded structure, undergoing displacive phase transitions. These minerals show a high initial rate of thermal expansion due to the progressive rotation of the tetrahedra. Thermal expansion coefficients become even larger just below the transformation temperature and then decrease abruptly to near zero when the fully-expanded structure is achieved. Quantitative calculations [8] show that the thermal expansion of quartz is due chiefly to tetrahedral rotations, with only a minor contribution from thermal motions.

Volume expansivity is equal to the sum of the linear expansion coefficients. For β -eucryptite, LiAlSiO₄, the coefficients are $\alpha_a = \alpha_b = 7.8 \times 10^{-6} \text{ K}^{-1}$, and $\alpha_c = -17.5 \times 10^{-6} \text{ K}^{-1}$. The volume expansivity is $-1.9 \times 10^{-6} \text{ K}^{-1}$, one of the few materials which becomes denser when heated. β -eucryptite has a quartz-like structure with aluminum replacing silicon and lithium occupying 4- or 6-coordinated sites in the *c*-axis

Table 7. Thermal expansion coefficients of the pseudobrookite structures. All coefficients expressed in units of $10^{-6}/^{\circ}\text{C}$

	α_a	α_b	α_c	
Al_2TiO_5	9.5	19.0	-1.4	CARTZ [9]
Fe_2TiO_5	10.9	16.3	3.0	CARTZ [9]
MgTi_2O_5	12.0	12.0	2.0	BUSH and HUMMEL [10]

channels. The unusual thermal expansion behavior has been attributed to a redistribution of lithium ions among the 4- and 6-fold sites. The cell volume decreases with increasing temperature as the number of Li^+ ions in 6-fold coordination increases. Calculations show that the observed expansion behavior up to 1000°C could be accounted for by switching 10–20% of the lithium from four to six-fold positions.

Layer and chain-type structures often exhibit highly anisotropic thermal expansion coefficients. The pseudobrookite structures contain chains of TiO_6 octahedra along c , chains which are bonded together by highly distorted Al polyhedra. The Al–O bond lengths range between 1.84 and 2.14 Å. Thermal expansion coefficients (Table 7) are greatest in the a – b plane, perpendicular to the Ti–O chains. The chains twist and separate with temperature but do not lengthen appreciably. The maximum Al–O bond length in the a – b plane corresponds to the minimum thermal expansion coefficient in the plane, so that bond lengths tend to become more equal with increasing temperatures.

Aluminum titanate, hafnium titanate and a few other oxides have negative thermal expansion coefficients in certain directions. The anisotropy in thermal expansion can be explained by distortions in the coordination polyhedra. With increasing temperature the atoms shift so as to minimize the distortions, as has been verified in β -spodumene ($\text{LiAlSi}_2\text{O}_6$) and Al_2TiO_5 . Ceramic specimens of these oxides show unusually low dilatometric expansivities and low mechanical strengths. Both properties result from intergranular microfractures caused by the anisotropy in thermal expansion.

MEGAW [7] has shown that α is inversely proportional to the square of the bond strength. Examples are given in Table 8 which show that the product αq^2 is approximately constant. The bond strength is defined as in Pauling's rules as valence divided by coordination number. It is reasonable to expect that stronger bonded materials will have smaller expansion coefficients. This accounts for the often made observation that materials with high melting points have low α values. All materials expand about 15% before melting.

Table 8. Relation between bond strength q and thermal expansion [11]

	q	α	αq^2
CsCl	1/8	53×10^{-6}	0.97×10^{-6}
NaCl	1/6	40×10^{-6}	1.11×10^{-6}
CaF_2	2/8	19×10^{-6}	1.19×10^{-6}
CuBr	1/4	19×10^{-6}	1.19×10^{-6}
MgO	2/6	10×10^{-6}	1.11×10^{-6}
ZrO_2	4/8	4.5×10^{-6}	1.12×10^{-6}

Although α depends mainly on bond strength, there are variations between isomorphous crystals. For example, thermal expansion coefficients for alkali halides with the rocksalt structure range from NaF $34 \times 10^{-6}/^{\circ}\text{C}$ to LiI $56 \times 10^{-6}/^{\circ}\text{C}$. Radius-ratio appears to be important since α is largest for LiI, LiBr, LiCl, NaI, and NaBr where r_+/r_- is small. Anion-anion repulsion loosens the structures making expansion easier. KHAN [12] has discussed the effect of ionic size on thermal expansion.

In molecular crystals, thermal expansion coefficients are also strongly influenced by geometrical factors. Lead azide, $\text{Pb}(\text{N}_3)_2$, is a primary explosive of considerable importance in military and industrial applications. In the orthorhombic α form, linear N_3^- azide ions are arranged in sheets perpendicular to the a -axis. These layers are separated by Pb^{2+} ions bonded to eight azide groups. Within the (001) sheets, the azide ions are nearly parallel to b and are linked end to end by lead atoms to form chains. Rotation of the azide groups with temperature will therefore enhance thermal expansion along a and c but not along b . Expansion along the a direction normal to the sheets is expected to be largest because of the weak interlayer bonding. The expected sizes of expansion coefficients is therefore $\alpha_b < \alpha_c < \alpha_a$, which is the order observed. Measured values [13] are $\alpha_a = 5.7 \times 10^{-5}$, $\alpha_b = 0.3 \times 10^{-5}$, and $\alpha_c = 1.4 \times 10^{-5} \text{ K}^{-1}$.

Thermal expansion of layer-type crystals is largest normal to the layer. In hydrocarbons and other planar molecular crystals, expansion is a maximum normal to the molecules. Expansion coefficients for crystalline benzene (-193° to -3°C) are 11.9, 10.6, and $22.1 \times 10^{-5}/^{\circ}\text{C}$ parallel to the a , b , and c orthorhombic axes. The C_6H_6 molecules in benzene lie close to the (001) plane, normal to the direction of largest expansion. The same is true of naphthalene (C_{10}H_8) and anthracene ($\text{C}_{14}\text{H}_{10}$). Expansion is greater for crystals with small molecules than for their larger homologs. The average thermal expansion coefficients for benzene, naphthalene, and anthracene are 14.7, 12.7, and $8.0 \times 10^{-5}/^{\circ}\text{C}$ [2].

The thermal expansion coefficient of Invar alloys is nearly zero over a broad temperature range below the ferromagnetic Curie point. A magnetically-induced contraction offsets normal thermal expansion to produce this useful effect. Magnetic dilation falls to zero just above T_c where magnetic short range order disappears. Therefore the temperature dependence of magnetic expansion is opposite in sign to that of the thermal expansion arising from increased amplitude of atomic vibrations. The magnetic contribution depends on the type of magnetic exchange interaction as well as the degree of magnetic order. Magneto-elastic contractions are especially intense for ferromagnetic exchange interactions because ferromagnetic ordering eliminates d -electron bonding between atoms. The Pauli exclusion principle excludes electron transfer between two half-filled orbitals of parallel spin. At low temperatures where ferromagnetic order is complete, there is no d -electron bonding, enlarging interatomic distances. With increasing temperature, thermal vibration increases, along with magnetic disorder. The lattice expansion caused by increased vibration is cancelled by a contraction resulting from increased d -electron bonding. The net result is a material with very low thermal expansion. Alloy composition can be adjusted to give complete compensation. Antiferromagnetic interactions generally enhance d -electron bonding.

Variation in thermal expansion coefficients with composition have been used to strengthen polycrystalline ceramic bodies. Alumina and other refractory oxides have been chemically strengthened by forming solid solution surface layers at high temperatures. If the surface layer has a low expansion coefficient, the interior contracts more than the surface, placing the surface layers in compression. Additional improvements in the mechanical properties is achieved by eliminating localized stresses which arise because of anisotropy in the thermal expansion. Little stress is present in a ceramic of randomly oriented anisotropic crystals when sintered at high temperatures. During cooling, however, individual grains contract more in the high expansion directions, giving rise to localized stresses at the grain boundaries. Such effects can be eliminated by choosing a solid-solution composition for which thermal expansion is isotropic.

6. Diffusion

Heat capacity and most other bulk properties are insensitive to defect concentration but this is not true for transport properties such as diffusion. Diffusion often controls solid-state reactions and is important in a number of chemical and metallurgical problems. The diffusion coefficient D relates the flux of diffusing atoms to their concentration

gradient. D is extremely temperature-sensitive since most diffusion processes are thermally activated. At elevated temperatures, thermal vibration increases in amplitude leading to atom transport and diffusion, usually by one of the processes illustrated in Fig. 25. The *ring* and *interchange* mechanisms are more important in metals than in ion solids because an exchange of neighboring cations and anions requires a great deal of energy. *Vacancy* and *interstitial* processes require less energy than interchange because only one atom is misplaced, rather than two or more. Diffusion *via* vacancies requires a neighboring lattice vacancy and therefore tends to be less rapid than the interstitial mechanism. Atom sizes

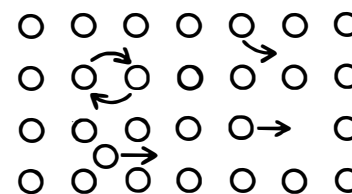


Fig. 25. Four diffusion mechanisms: interchange, vacancy, interstitial, and dissociative

are very important, with small atoms like hydrogen and carbon diffusing rapidly *via* interstitial sites in many metals. Thus D depends on the nature of the diffusion atom and the host lattice. For rapid diffusion, the host lattice must provide suitable interstitial sites and the "necking down" between sites must not be excessive. Zeolites are ideal from this point of view, with many cavities connected by open channels, making them useful in ion-exchange applications.

A number of interesting phenomena involve the movement of atoms from one site to another under the driving force of temperature gradients, concentration gradients, mechanical stress, or electric fields. Sintering and grain growth are controlled by diffusion, as are ionic conductivity, metal oxidation, high-temperature creep, and dielectric loss in glass.

In compounds, different ion species often diffuse at vastly different rates, although electrical neutrality requires that the diffusion rates be coupled. Diffusion coefficients for simple oxides are shown in Fig. 26. Thermal vibration assists diffusion, causing the increase in D with temperature. Multiple-valence transition metals have high diffusion rates because of the importance of defects. The diffusion coefficients of the large oxygen ions are small except for calcium-stabilized zirconia which contains anion vacancies.

Most practical materials are polycrystalline rather than single crystals. The mechanical strength and certain other properties of metals

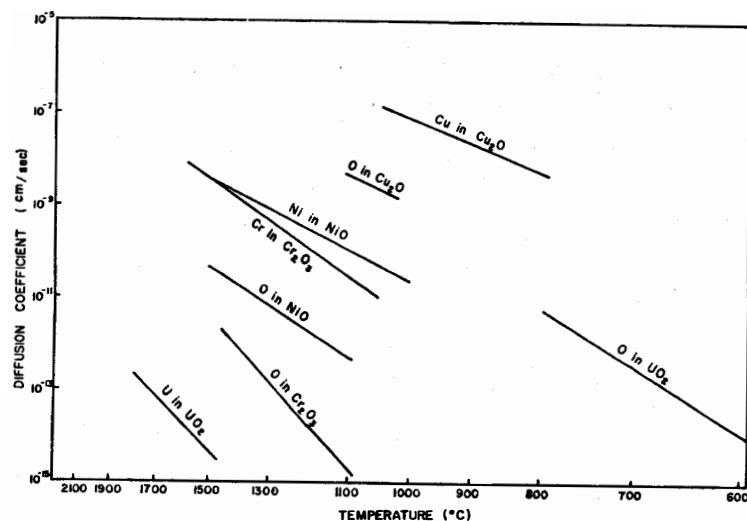


Fig. 26. Diffusion coefficients for cations and anions in several oxides. Generally the cations diffuse faster than oxygen, although there are exceptions such as uraninite [14]

and ceramics are improved by making such materials as dense as possible by reducing the pore space between crystallites. During the sintering process, temperature and sometimes pressure are used to join the particles. Understanding of the sintering process has advanced rapidly during the past decade with the realization of the importance of diffusion processes. It is now possible to prepare many polycrystalline bodies to within a few percent of theoretical (single crystal) density. This has led to the development of new products such as Lucalox, a transparent corundum ceramic [14].

Most ceramics are opaque because included pores scatter light. Pores can be eliminated by control of the sintering process, giving alumina ceramics which transmit 90% of the incident light. The chemical inertness and high melting point of transparent alumina have led to the development of new high-intensity sodium-vapor lamps with a continuous spectrum and a luminous efficiency vastly superior to incandescent and fluorescent lamps. Pore-free alumina is not, however, completely transparent because each grain is birefringent and each boundary is a light-scattering interface.

There are several stages in the sintering process: 1. irregular shaped particles are rounded, 2. necking between particles, 3. widening of the

necks, 4. grain growth. Pore sizes decrease during sintering, ending with a few pores trapped within individual grains.

Two key ideas are involved in understanding and controlling the sintering process. The first is that surface energy is the driving force behind the sintering process. Surface free energy is minimized by minimizing surface area. Thus the various stages in sintering each correspond to a reduction in surface area, first in particle shape, then in pore volume, and finally in grain volume. Highly curved areas such as the neck between particles grows faster than other regions because of the greater surface area.

The second important idea about sintering is that vacancies are generated in pores and diffuse to grain boundaries. At the same time atoms diffuse in the opposite direction, reducing the pore size. Sintering is basically a diffusion-controlled process in which the diffusion coefficients and distances between pores and grain boundaries are crucial.

In attempting to reduce sintering time, particle size reduction helps immensely. The diffusion distance between pores and grain boundaries is shorter in small grains so that sintering time is proportional to particle volume.

Crystal chemistry is helpful in controlling diffusion coefficients. Rapid sintering calls for large diffusion coefficients, but it is important to realize that *all* atoms must be transported. Thus the most important diffusion coefficient is the smallest diffusion coefficient, the rate-limiting coefficient. In oxides and similar materials, the anion usually has the smallest coefficient because it is usually larger than the cations. Anion diffusion can be increased by introducing anion vacancies. There are several ways of doing this. Doping the material with cations of smaller valence (Li_2O in MgO) or anions of higher valence (oxygen in a fluoride) are two chemical methods. Aluminum oxide can be sintered to theoretical density by adding about 0.1% MgO in solid solution. Another related technique is to heat the material in a reducing atmosphere.

Atomic migration in solids can be stimulated by light and infrared radiation [15]. Control of the diffusion process by high-power lasers may be directional in certain systems, an effect which could be utilized in certain applications. For instance, ultra-high purities might be attained by driving out impurities with laser-excited phonons. Laser-stimulated diffusion could also be used to achieve complex dopant profiles by adjusting the wavelengths, directions, and intensities of incident laser beams. High power density, such as that supplied by Q-switched ruby lasers, is required for stimulated diffusion.

To participate in directional diffusion, the phonons must have a wave vector and branch suitable to induce opposing motions in neighboring atoms. Phonons are created by Raman scattering processes or by photon

absorption at defect or impurities. Internal bulk damage, such as bubble formation and damage tracks, may be attributable to such processes. Damage occurs at power densities near 10^{10} W/cm² in glass, ruby, and other solid state laser materials. Point defects created by the beam diffuse together to form long microcracks. The reorientation of color centers provides a second example. F_A centers in sodium-doped KCl consist of a Na substitutional impurity adjacent to an F-center. At low temperatures, the centers can be reoriented by exciting the appropriate phonons.

7. Ionic Conductivity

In ceramics, the electrical conductivity associated with ion motion may exceed electronic conductivity by several orders of magnitude. Diffusion and ionic conductivity (σ) are related through the Nernst-Einstein equation:

$$\sigma = \frac{Dnq^2}{kT}$$

Here n is the number of charge carriers per unit volume, q the charge per ion, k is Boltzmann's constant, and T the absolute temperature. The diffusion coefficient (D) generally refers to the more rapidly moving species but there are many ambiguities in the use of this relation, especially for direct current measurements. Diffusion generally occurs by the movement of ions to neighboring vacancies. For stoichiometric compounds, the vacancy concentration and ionic conductivity are very small, although suitable doping will increase both.

Impurities and other defects often play a decisive role in electrolytic conduction. In a salt crystal, the movable charges may be interstitial ions (Frenkel defects) or vacancies (Schottky defects). The position of a vacancy changes when a neighboring ion moves in to fill it. Schottky defects predominate in KCl where both cation and anion vacancies occur. In AgCl, some Ag^+ ions occupy interstitial sites producing positive Frenkel defects and negative Schottky defects.

Charges are transported by mobile protons in ice. Each H_2O molecule in the ice structure is surrounded by four neighboring molecules at 2.76 Å. Hydrogens lie near lines joining adjacent oxygens and are closer to one than the other. The distances are about 1.0 and 1.8 Å. Two neutrality conditions are normally satisfied. Water molecules are generally intact and neutral with two hydrogens near each oxygen. The second condition pertains to the integrity of the hydrogen-bonding network. One and only one hydrogen connects any two neighboring oxygen

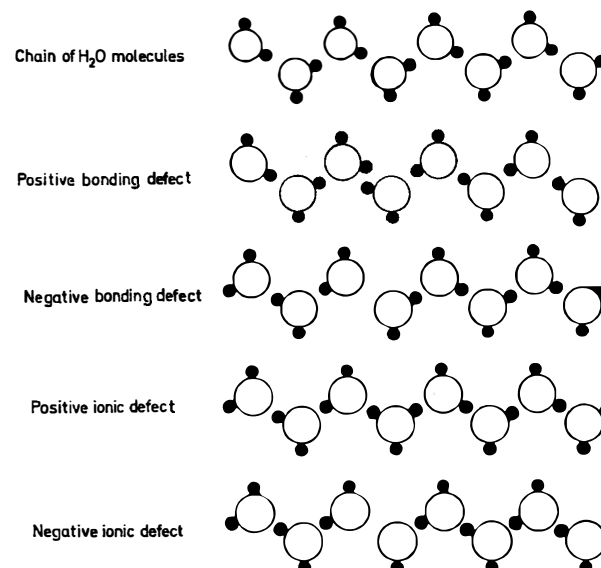


Fig. 27. Molecular chains in ice and four types of electrically-active defects

ions. Violation of either neutrality rule produces an electrically-active defect.

Several electrically-active defects in ice are illustrated in Fig. 27. Rotation of one molecule causes a pair of defects: a positive bonding defect with 2H on the same bond, and a negative bonding defect with none. The positive and negative can separate and move through the crystal by successive rotation of neighboring molecules. Two other defects occur when a proton is transferred from one molecule to another, creating positive hydronium H_3O^+ and negative hydroxyl OH^- . Hydronium moves by donating a proton to an adjacent molecule. Hydroxyl moves by capturing a proton from a neighboring water molecule.

The motion of hydronium and hydroxyl ions leaves molecules oriented against the field, with the molecular dipole moment anti-parallel to the applied field. Passing bonding defects leaves the molecular dipoles parallel to the field. Bonding defects dominate the polarization in pure ice because they are much more numerous than ionic defects. Bonding defect concentrations are about 10^{-6} .

Charge transport of direct current in pure ice is about equally divided between bonding and ionic defects. Ionic defects are fewer in number but

somewhat higher in mobility. Each type of defect carries about half an electronic charge [16].

Quartz has a relatively open structure with channels along the trigonal *c*-axis, causing anisotropy in the electrical conductivity. In directions normal to the *c*-axis, quartz is a good insulator, but parallel to *c*, conduction of an electrolytic nature occurs readily. Ionic conduction may involve impurity ions already in the structure, or deliberately-introduced foreign ions. At 250° C, Na⁺ ions are easily transported through the crystal from a sodium amalgam anode, but K⁺ ions from a potassium amalgam anode pass through with much less facility. Activation energies for diffusion increase steadily with ionic radius, ranging from 18 kcal/mol for Li⁺ (0.6 Å radius) to 33 kcal/mol for Cs⁺ (1.7 Å). Passage through the *c*-axis channels becomes increasingly difficult for ions exceeding the channel diameter in size. The behavior of Ag⁺ ions in quartz is especially interesting because of the visible silver deposits left behind. Thread-like formations parallel to *c*, and platelets perpendicular to *c* are observed [17].

8. Ionic Switches

Materials showing bistable switching satisfy three basic requirements [18]: 1. electrical conductivity increases with temperature, 2. the initial conductivity is large enough to produce localized heating at reasonable electric fields, and 3. the heating promotes a reversible structural or compositional change which produces the conductive state. Electronic switches are well known but ionic threshold switching has also been observed [19] in AgI, CuBr · 2H₂O, and SnCl₂ · 2H₂O.

The ionic conductivity of silver iodide increases abruptly by almost three orders of magnitude at the hexagonal-cubic phase transition. Under small applied voltages, the temperature rises slowly to the transition at 146° C. Filaments of the high-temperature phase form rapidly at the transition, rapidly lowering the resistivity so that a sudden decrease in voltage and switching results. The reproducibility of the current-voltage characteristic is strongly dependent on repetition frequency.

Dehydration of NaBr · 2H₂O crystals at 51° C also produces switching. Near the transition, dehydration filaments fill with a conductive solution of NaBr in water, increasing the conductivity. When the electric field is reduced crystals reform into the initial high-resistance state.

Switching can occur during melting, as in stannous dichloride dihydrate. The compound melts at 38° C without dehydration into a conducting liquid. The switching behavior of SnCl₂ · 2H₂O is more reproducible than NaBr · 2H₂O because no water is lost during the transformation.

9. Superionic Conductors

There are a few solids which have ionic conductivities comparable to liquids. At room temperature, aqueous electrolytes have conductivities near 1 Ω⁻¹ cm⁻¹, while non-aqueous electrolytes are generally somewhat lower. Two of the best solid ionic conductors are RbAg₄I₅ and NaAl₁₁O₁₇, which are rather open structures in which cations diffuse rapidly. The room temperature conductivities of these compounds lie between 10⁻¹ and 10⁻² Ω⁻¹ cm⁻¹. Anions will also diffuse but with greater difficulty because of their larger size. At 1000° C, rapidly moving oxygen ions increase the conductivity of defect solid solutions in the ZrO₂-Y₂O₃ system to as high as 10⁻¹ Ω⁻¹ cm⁻¹.

Superionic conductors exhibit very high ionic conductivity with negligibly small electronic conductivity. Three main groups of superionic conductors are listed in Table 9. The silver halide group is characterized by cation disorder, as are the beta-alumina structures. In both these groups the univalent cations Ag⁺, Na⁺, Cu⁺ are especially mobile. Oxygens are the conducting species in the defect-stabilized oxide group. In calcia-stabilized zirconia, calcium introduces a large number of anion vacancies into zirconia as indicated by the formula Ca_x²⁺Zr_{1-x}⁴⁺O_{2-x}²⁻□_x.

The ionic conductivity of RbAg₄I₅ near room temperature is about 17 orders of magnitude larger than that of NaCl. The activation energies

Beta-alumina A₂O · nM₂O₃

are small, since the large conductivities are attained well below the melting point of the superionic conductor. Such materials contain a large number of mobile charge carriers which is independent of temperature. Schottky or Frenkel defects are responsible for ionic conductivity in ordinary ionic compounds, so that the number of charge carriers is small and temperature dependent. Not only is the number of carriers large in a superionic conductor, but the mean free paths may be large as well. In the stabilized zirconia group, mobile oxygen ions are transported over many interatomic distances by a cooperative mechanism. In conventional ionic conductors the mean free path is one "hop" between neighboring ions.

Several silver halides are excellent solid electrolytes with conductivities approaching those of liquid electrolytes. The silver ions occupy interconnected passageways formed by face-sharing anion polyhedra. The number of polyhedra exceeds the number of mobile cations. In α -AgI and other electrolytes based on a body-centered cubic arrangement of iodine atoms, the anions form passageways of face-sharing tetrahedra. The α -Ag₂HgI₄ structure consists of a face-centered cubic arrangement of iodine atoms with silver ions moving through passageways formed by face-sharing octahedra and tetrahedra. In the more complex RbAg₄I₅ and [(CH₃)₄N]₂Ag₁₃I₁₅ structures [21], the passageways are made up of face-sharing tetrahedra, while in (C₅H₅NH)Ag₅I₆ the silver ions occupy channels of iodine octahedra and tetrahedra. At low temperatures Ag⁺ occupies two of the three crystallographically-independent positions, with the third site empty. All three positions are partially occupied at room temperature, showing that conductivity involves the thermal excitation of silver ions into empty polyhedra.

A theory for superionic conductors has recently been advanced by RICE and ROTH [20]. According to their model, ions can be excited from a stationary ground state across a threshold energy to a continuum of excited states in which the ions are mobile. The excitation has a characteristic life-time τ related to its velocity v and mean free path l by $l = v\tau$.

A domain model for anomalously fast diffusion has been described by VAN GOOL and BOTTELBERGHS [22]. The basic idea of the domain model can be illustrated with Na₂O · 11Al₂O₃, sometimes referred to as β -alumina. The structure consists of spinel-type layers separated by Na-O layers. The oxygen functions as spacers between the spinel blocks as sodium migrates easily (Fig. 28). Sodium ions are found in two different sites, leading to two different structures when Na is assigned to one set of sites or the other. Electrostatic calculations show that the energy differences between the two structures are small, suggesting the possibility

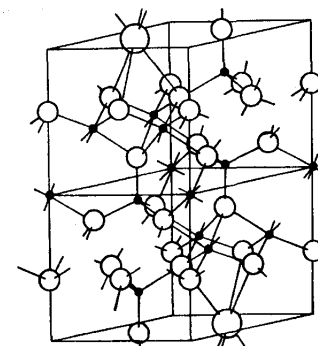


Fig. 28. A perspective drawing of half of the unit cell of β -alumina. The large circles represent Na, the small ones oxygen, and the black dots aluminum atoms

of fluctuating domains in the material. Cooperative displacement of neighboring Na⁺ ions leads to domain wall motion, a possible mechanism for superionic conductivity.

10. Solid State Battery Materials

The advent of nuclear power, the impending replacement of the internal combustion engine, and bioengineering applications all point to the need for electrochemical power sources—small solid-state batteries with high power densities and high-energy densities. To keep the weight down, which for a battery is important for transportation applications, light elements are preferable but the prime requirement is high ionic conductivity.

The *electrolyte* of a battery should be a good ionic conductor and a good electronic insulator. Looking to the future, materials with open structures are an obvious choice to promote rapid ion diffusion. These may be one-dimensional channels, as in the tungsten bronzes, beryl, or quartz; two-dimensional widely spaced layers as in graphite, BN or β -alumina; or three-dimensional interconnected channels as in the zeolites or certain borides.

In the sodium-sulfur storage battery, molten sodium is separated from molten sulfur by a beta-alumina ceramic. The overall reaction ($\text{Na} + x\text{S} \rightarrow \text{NaS}_x$) produces a cell potential exceeding two volts, and far surpasses the lead acid battery in its energy to weight ratio.

Solid state battery *electrodes* must not only be good ionic conductors but good electronic conductors as well. The tungsten bronzes appear

especially attractive because they are open structures in which ions can diffuse, and the mixed valence of the tungsten ions promotes rapid electron transfer.

11. Photographic Process

The photographic process is closely related to superionic conductivity. Silver bromide is converted to particles of black metallic silver by light. When light is incident upon the film, electron-hole pairs are created. The rapidly moving electrons migrate to metallic silver nuclei under the action of image forces, and the tiny metallic particles therefore become negatively charged. The negatively charged nuclei set up electrostatic fields within the silver bromide crystal, causing Ag^+ ions to drift toward the metal. When they reach the metal, the cations neutralize the negative charge and neutral silver atoms are added to the metal nuclei causing them to grow. Silver ions are very mobile in AgBr because of the cation disorder in which large numbers of silver atoms are in interstitial positions. The holes created by light drift slowly to the surface of the AgBr crystal where bromide ions are neutralized and bromine molecules liberated.

Photosensitization is important in silver halide photography and in electrophotographic processes such as the zinc oxide Electrofax system. In the process of spectral sensitization, a dye is placed in contact with a solid, resulting in advantageous photoelectric or chemical effects [23]. Colors can be sensed by a dye-sensitized solid which can then be used in vidicons and other photoelectric devices.

Spectral sensitization by dyes is observed in Ge , Se , TiCl , CdS , ZnO and many other photoconducting elements. Anionic dyes (fluorescein, eosin), cationic dyes (malachite green, fuchsin), and neutral dyes (chlorophyll, phthyanines) of different classes can all produce electrical effects. For good sensitizing activity, the dye must be strongly adsorbed on the surface of the solid. The adsorption condition together with the behavior of thick dye layers and the regeneration of photoionized dyes suggest that charge-transfer is the dominant mechanism in dye-photoconductor systems. Free electrons or holes are produced in the solid as a consequence of photon absorption by the dye. The relative positions of the electron energy levels of the dye and the photoconductor is a key feature of photosensitization. Electron transfer occurs when the lowest vacant level of the dye is situated above the conduction band of the photoconductor. The dye absorbs a photon, raising an electron to an excited state, and the electron is subsequently injected into the conduction band of the solid. Hole transfer takes place when the highest occupied energy

level of the dye is below the valence band of the semiconductor. The sign of the charge carriers in sensitized photoeffects is generally the same as that of the intrinsic photoeffect of the solid.

12. Thermoelectric Materials

Thermoelectric materials have found varied uses as refrigerators, radiation thermopiles, oil burner generators, solar converters and hygrometers. All such devices involve the conversion of heat to electricity or the reverse process [24]. Additional applications await the discovery of materials with a higher thermoelectric figure of merit, $z = \alpha^2 \sigma / K$. The electric and thermal conductivities are σ and K , and α is the Seebeck coefficient, the potential difference developed as a result of a temperature difference between the junctions of two conductors.

The Seebeck coefficients of more than $1 \text{ mV}/^\circ\text{C}$ have been found in semiconductors, making them superior to metals as thermoelectric elements. The product, $\alpha^2 \sigma$, is largest for semiconductors operated in the extrinsic range, with band gaps of at least $6kT$, 0.15 eV at room temperature. Carrier mobility and effective mass should be high, and the lattice component of the thermal conductivity low. The latter is achieved using heavy elements and solid solutions to promote phonon scattering. Alloys based on bismuth telluride, Bi_2Te_3 , exhibit high figures of merit.

It is also advantageous for the materials to withstand high temperatures because high efficiencies require large temperature differences between junctions.

13. Thermionic Materials

A heated cathode emits electrons giving rise to an emission current which can be collected and measured [25]. The work function is a measure of the escape energy. Low work functions are desirable in many electronic applications. Among the elements, the easily-ionized alkali metals have especially low work functions, near 2 eV . These metals are not very stable, however, and substitutes have long been sought.

Among the more promising replacements are the rare earth borides, especially YB_6 and LaB_6 which are used as cathodes in high-power generator devices. The hexaborides have low work functions (about 2.5 eV), and are stable in high and low vacuums at 1500°C under ionic bombardment and high electric fields. Lanthanum metal does not have a low work function, and it is believed that the La donates electrons to the boron complex (Fig. 29), from which they are readily boiled off when

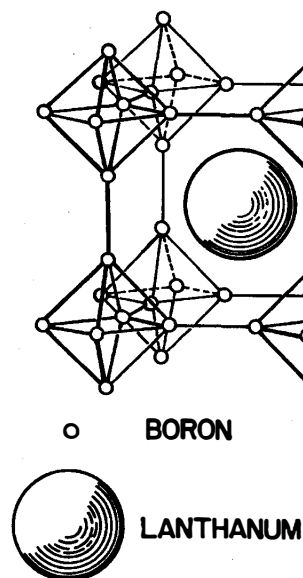


Fig. 29. A number of hexaborides have the LaB_6 structure in which lanthanum atoms occupy cubo-octahedral interstices between interconnected boron octahedra

heated. LaB_6 has a lower work function than the other rare earth borides because the outer electrons are more easily ionized, being d and s electrons, rather than f electrons.

References for Chapter III

1. LONSDALE, K.: Crystals and X-rays. Princeton, N.J.: D. Van Nostrand Co. 1949.
2. International tables for X-ray crystallography, Vol. III. Birmingham, England: Kynoch Press 1962.
3. BRILLOUIN, L.: Wave propagation in periodic structures. New York: Dover Publications 1953.
4. FLEURY, P.A.: In: CROSS, L.E. (Ed.): Phase transitions-1973, p. 195. New York: Pergamon Press 1973.
5. OLIVER, D.W., SLACK, G.A.: J. Appl. Phys. **37**, 1542 (1966).
6. LEWIS, M.E., PATTERSON, E.: J. Appl. Phys. **44**, 10 (1973).
7. MEGAW, H.D.: Mat. Res. Bull. **6**, 1007 (1971).
8. TAYLOR, D.: Min. Mag. **38**, 593 (1972).
9. CARTZ, L.: In: VAHLDIRK, F.W., MERSEL, S.A. (Eds.): Anisotropy in single crystal refractory compounds, Vol. 1, p. 388. New York: Plenum Press 1968.

10. BUSH, E.A., HUMMEL, F.A.: J. Am. Ceram. Soc. **42**, 388 (1959).
11. MEGAW, H.D.: Z. Krist. **100**, 58 (1938).
12. KHAN, A.A.: Acta Cryst. A **30**, 105 (1974).
13. MAUER, F.A., HUBBARD, C.R., HAHN, T.A.: J. Chem. Phys. **60**, 1341 (1974).
14. BURKE, J.E.: Science **161**, 1205 (1968).
15. FRANKLIN, W.M., SANGUPTA, P.: Trans. I.E.E.E. QE-8, 393 (1972).
16. ONSAGER, L.: J. Chem. Phys. **50**, 1089 (1969).
17. WHITE, S.: Nature (London) **225**, 375 (1970).
18. COOK, E.L.: J. Appl. Phys. **41**, 551 (1970).
19. OGORELEC, Z.: Sol. State Commun. **14**, 65 (1974).
20. RICE, M.J., ROTH, W.L.: J. Sol. State Chem. **4**, 294 (1972).
21. GELLER, S.: Science **176**, 1016 (1972).
22. VAN GOOL, W., BOTTELBERGHS, P.H.: J. Sol. State Chem. **7**, 59 (1973).
23. MEIER, H.: Photochem. and Photobiol. **16**, 219 (1972).
24. GOLDSCHMIDT, H.J.: Applications of thermoelectricity. London: Methuen and Co. 1960.
25. SAMSONOV, G.V.: High temperature compounds of rare earth metals with nonmetals. New York: Consultants Bureau 1965.